



**HAL**  
open science

## Effects of biofuel from fish oil industrial residue - Diesel blends in diesel engine

Nadia Mrad, Edwin Geo Varuvel, Mohand Tazerout, Fethi Aloui

► **To cite this version:**

Nadia Mrad, Edwin Geo Varuvel, Mohand Tazerout, Fethi Aloui. Effects of biofuel from fish oil industrial residue - Diesel blends in diesel engine. *Energy*, 2012, 44 (1), pp.955-963. 10.1016/j.energy.2012.04.056 . hal-00935914

**HAL Id: hal-00935914**

**<https://hal.science/hal-00935914>**

Submitted on 22 Jun 2021

**HAL** is a multi-disciplinary open access archive for the deposit and dissemination of scientific research documents, whether they are published or not. The documents may come from teaching and research institutions in France or abroad, or from public or private research centers.

L'archive ouverte pluridisciplinaire **HAL**, est destinée au dépôt et à la diffusion de documents scientifiques de niveau recherche, publiés ou non, émanant des établissements d'enseignement et de recherche français ou étrangers, des laboratoires publics ou privés.



Distributed under a Creative Commons Attribution 4.0 International License

# Effects of biofuel from fish oil industrial residue – Diesel blends in diesel engine

Nadia Mrad<sup>a</sup>, Edwin Geo Varuvel<sup>a,\*</sup>, Mohand Tazerout<sup>a</sup>, Fethi Aloui<sup>b</sup>

<sup>a</sup>École des Mines de Nantes, Département Systèmes Énergétiques et Environnement (DSEE), GEPEA, CNRS-UMR 6144, 4 rue Alfred Kastler, BP20722, 44307 Nantes Cedex 03, France

<sup>b</sup>Université de Valenciennes, ENSIAME, TEMPO – EA4542 (DF2T), Le Mont Houy, F-59300 Valenciennes Cedex 9, France

The present work aims to produce biofuel from fish oil industrial residue and to test the biofuel in diesel engine. A 4.5 kW at 1500 rpm single cylinder air cooled direct injection diesel engine was used for the present experimental work. The experimental results show that the brake thermal efficiency marginally increases with biofuel from 29.98% (neat diesel) to the maximum of 32.4% with biofuel at 80% of maximum load. Also experiments were conducted with different blends of biofuel and diesel (B20 and B40). Though the NO<sub>x</sub> emissions are high with neat biofuel and blends, the other emissions like CO, HC and particulate matter (PM) are decreased. The PM emissions decrease when the percentage biofuel increases in the blend. It reduces from 8271 ng/s with neat diesel to 8137 ng/s with B40. It further reduces to the minimum of 7842 ng/s with neat biofuel. The cylinder peak pressure increases as the biofuel quantity increases in the blend. The rate of premixed combustion increases with neat biofuel and its blends than neat diesel. Addition of biofuel with diesel decreases the combustion duration and ignition delay due to higher cetane number of biofuel.

## 1. Introduction

Depletion of fossil fuels and environmental degradation are two major problems faced by the world. Today fossil fuels take up to 80% of the primary energy consumed in the world, of which 58% alone is consumed by the transport sector [1]. Increasing energy demand leads to increase in crude oil price, directly affected to global economic activity [2]. A country's development is strongly linked to the availability of fuels for transportation and power generation. Thus, world faces the major challenge of high oil demand to meet the growing energy needs. It is important to explore alternative, renewable, sustainable, efficient and cost-effective energy sources which can be produced with in the country on a massive scale for commercial utilization.

Finding suitable substitutes for the petroleum based fuels have gained importance during the recent years [3–5]. Biofuels have emerged as one of the most important sustainable fuels in the foreseeable future. Biofuels are referred to liquid, gas and solid fuels produced from biomass. Liquid fuels because of their high energy content per unit volume and ease of handling and distribution are better suited as compared to solid and gaseous fuels. The prime liquid alternative fuels are alcohols, biodiesel and biofuel through biomass waste. Alcohols are derived from bio-matter such as corn,

sugar cane or grain is frequent, this will often be referred to as bio-ethanol and can substitute for gasoline in spark-ignition engines and it is very difficult to use in diesel engine because of low cetane number, low calorific value, high latent heat of vaporization and high self ignition temperature [6,7]. Now a days, alcohols and biodiesels are produced through food crops [8,9]. Hence, the competition between foods vs. fuel may occur and also the cost involved for the raw materials increase the total cost of biodiesel production.

Biomass waste is one of the most promising alternative energy sources as it is renewable, widely available and contains much less sulfur and nitrogen [10]. Among the various biomass waste sources, industrial oil and fat waste have attracted much attention as candidates for alternative fuels and a great deal of research has been conducted on their feasibility as an alternative to diesel fuel. Thus, extensive literature is available on evaluation of biofuel from waste as diesel engine fuel [11–14].

A variety of different process designs have been proposed for the production of biofuel from biomass waste [15–18]. Among the various methods, thermo-chemical process is the most promising method for converting crude waste oil or fat (unpurified) to biofuel. Pyrolysis and catalytic cracking are two commonly utilized thermo-chemical conversion techniques. Each process generates products of solid, liquid and gas from a wide range of waste materials including fats and grease [19,20]. The relative proportions of products depend very much on the process method and reactor process parameters. The liquid phase, evolved during pyrolysis and

\* Corresponding author. Tel.: +33 0 2 51 85 82 88; fax: +33 0 2 51 85 82 99.  
E-mail address: ve\_geo@yahoo.com (E.G. Varuvel).

catalytic cracking, is composed of a complex mixture of hydrocarbons with different chemical groups and molecular sizes [21,22] and can be used as fuel after upgrading.

In the present work the biofuel from fish oil industrial residue is produced by catalytic cracking. From the fish production, about 54% is transformed into waste i.e. offal, bones, skin/scales, etc. The wastes include heads, bones, tail etc which go to make the fish oil. These wastes contain 54% water, 4% solid and 42% fish oil (15% of total mass). To produce edible fish oil, the fish was treated by a series of processes, starting with cooking it thoroughly in boiling water, pressure it and centrifugation of the product to separate the crude oil, water and other impurities. The crude oil undergone a filtration by winterization to make it limpid by removing the waxes or fats naturally contained. The residue of the fish oil is called as waste fish fat (WFF). The WFF, residue of this treatment represents 4000 tonne/year, which is totally composed of triglyceride. The feedstock (waste fish fat) used in this study was obtained from SIRH group specialized in vegetable, animal and marine oils located in north of France. This waste is the residue of marine oil treatment which is brown in color and was used without any special purification treatment. The typical fatty acid composition has been analyzed by gas chromatography analysis (GC/FID) which is given in Table 1.

This paper aims to find the effect of minimum usage of biofuel which is produced from fish oil industrial residue with diesel fuel in diesel engine. The experiments were conducted with neat biofuel, B20 (20% of biofuel and 80% of diesel) and B40 (40% of biofuel and 60% of diesel) to find the suitability in diesel engine through performance, emission and combustion characteristics. Finally, the measured values of biofuel and their blends were compared with base diesel fuel.

## 2. Biofuel preparation and analysis

### 2.1. Catalytic cracking of WFF

In the present work, the catalytic cracking of waste fish fat was carried out at temperatures ranging from 350 °C to 480 °C with a slow heating rate of 2–3 °C/min using a laboratory scale reactor. The fat was introduced in the reactor and heated by an external electric resistance. The catalyst was placed just above the fat on a bed with small holes. When the temperature inside the reactor reaches 350 °C, the reaction starts. The generated vapor was passed directly over the catalyst surface, before leaving through the top of the reactor. Then it enters in a water cooled, counter flow, heat exchange which was kept at 10–15 °C. As a result, three fractions of

liquids were collected in the flask: the first is the pyrolysis water, and the second liquid fraction recovered until the temperature reaches 400 °C. The last fraction is the bio-oil recovered from 400 °C to 480 °C. After acidity analysis, it is found that the second fraction is so acidic (Acid value equal to 20 mg<sub>KOH</sub>/g) compared to the third one (Acid value equal to 0.8 mg<sub>KOH</sub>/g). For this, the main interest is focused on third fraction which is called biofuel. The flash point of biofuel is very low (27 °C) compared to the diesel fuel (56 °C). The volatile compounds reflects low flash point of biofuel. Hence, distillation was performed to extract the most volatile hydrocarbons from biofuel. After distillation, the flash point of biofuel (57 °C) is similar to diesel fuel.

### 2.2. Biofuel properties and analysis

The acid value is a measure of the amount of carboxylic acid and it was determined by titration with KOH/C<sub>2</sub>H<sub>5</sub>OH solution using phenolphthalein as an indicator. The samples were dissolved in a mixture of ethyl alcohol and diethyl ether (molar ratio 1:1) and the acid groups were neutralized with KOH/C<sub>2</sub>H<sub>5</sub>OH solution. The mass of the liquid sample from the bio-oil and the volume of the KOH/C<sub>2</sub>H<sub>5</sub>OH were used to calculate the amount of carboxylic acid. To estimate the dynamic viscosity, a SV10 Vibro Viscometer was used. The density of the bio-oil was estimated with a pycnometer. The elemental compositions of the main elements in the biofuel (carbon, hydrogen, nitrogen and oxygen) were determined using an Elemental Analyzer (Flash EA 1112, CE Instruments). The gross heating value was measured using an oxygen bomb calorimeter (model 6200, Parr Instruments Company). The flash point was measured using an automated Pensky–Martens model NPM 440, following the guidelines of the ASTM D93. All the properties of biofuel, diesel and the standard test methods used are given in Table 2.

The biofuel contains a large number of components of liquid hydrocarbons and in order to identify its composition a CG/MS (Gas chromatography/mass spectrometry) analysis was carried out. For this purpose a Perkin Elmer Turbo Mass Gold Mass Spectrometer coupled with a gas chromatograph CLARUS 500 was used. The column was SBLTM-5ms Capillary type, 30 m in length and 0.25 mm in internal diameter. The detector temperature was fixed to 350 °C and the injector temperature was 250 °C. The results obtained in terms of the majority compounds of diesel and biofuel are summarized in Table 3.

## 3. Materials and methods

A single cylinder, four-stroke, air cooled, direct injection, constant speed, diesel engine developing power output of 4.5 kW

**Table 1**  
Important properties of the waste fish fat.

Properties	Waste fish fat
Visual aspect	Liquid at 60 °C, brown color, typical smell
Water content (%)	<0.05%
Flash point (°C)	318
High heating value (kJ/kg)	39,000
Kinematic viscosity (mm <sup>2</sup> /s)	27
Density (Kg/m <sup>3</sup> )	893
Composition of fatty acids (%)	
Mysteric	1.05
Palmitoleic	5.00
Palmitic	16.00
Stearic	10.50
Oleic	45.60
Linoleic	20.60

**Table 2**  
Properties of biofuel and diesel.

Properties	Unit	Standard test method	Biofuel	Diesel fuel
Flash point	°C	ASTM D93-94	57	56
Acidity	mg <sub>KOH</sub> /g	ASTM D664	0.8	–
HHV	MJ/kg	ASTM D2015-85	45.10	45.71
Dynamic viscosity at 20 °C	Ns/m <sup>2</sup>	ASTM D7042	2.32	2.52
Density at 20 °C	Kg/m <sup>3</sup>	ASTM D4052-91	825	830
Kinematic viscosity at 20 °C	mm <sup>2</sup> /s	ASTM D445	1.7	2
Cetane number		ASTM D613	57	52
Cloud point	°C	ASTM D2500-91	9	–
Pour point	°C	ASTM D97-93	–5	–
Cold filter plugging point	°C	ASTM D6371	14	–

**Table 3**  
Major composition of biofuel and diesel.

Class	Hydrocarbons	
	Biofuel	Diesel
Alkene	1-Nonene	2,6-Dimethyle octane
	1-Decene	5-Ethyle-2-methyle heptane
	1-Undecene	3-Methyle-decane
	5-Undecene	5-Methyle-5-propyle nonane
	1-Dodecene	6-Methyle-dodecane
	2-Dodecene	5-Butyle-nonane
	1-Tridecene	2,10-Dimethyle undecane
	1-Tetradecene	2,7,10-Trimethyle dodecane
	1-Tetradecene	2-Methyle-tridecane
	7-Tetradecene	2-Methyle-tetradecane
	3-Hexadecene	2,6,10,14-Tetramethyle hexadecane
	1-Pentadecene	7-Methyle-pentadecane
	3-Octadecene	4-Methyle-tetradecane
		3-Methyle-tetradecane
		2,5-Dimethyle tetradecane
		2,6,10-Trimethyle tetradecane
		2,6,10,14-Tetramethyle pentadecane
		2,6,10-Trimethyle pentadecane
		2,6,10,14-Tetramethyle hexadecane
	2-Methyle-heptadecane	
Alkane	Nonane	Decane
	Decane	Undecane
	Undecane	Dodecane
	Dodecane	Tetradecane
	Tetradecane	Pentadecane
	Hexadecane	Hexadecane
	Cyclohexadecane	Heptadecane
	Heptadecane	Octadecane
	Octadecane	Nonadecane
	Nonadecane	Eicosane
	Eicosane	Docosane
	Heneicosane	Tricosane
		Tetracosane
	Heptacosane	
	Heneicosane	
Cyclo-alkane	1,2-Dimethyle-cyclooctane	Methylecyclohexane
	Cyclopentadecane	1-Methyle-3-propyle cyclohexane
	2-Cyclohexyl-undecane	Butyle cyclohexane
	Cyclohexadecane	Decahydro naphthalene
	Hexyl-cyclohexane	
	Heptylcyclohexane	
	4-Cyclohexyl-dodecane	
Aromatique	o-Ethyle-toluene	1,3,5-Trimethyle benzene
		1,2,3,4-Tetrahydro-2,7-dimethyle naphthalene
		3,3-Dimethyle-butyle benzene
		1,2,3,4-Tetrahydro-5-methyle naphthalene
		2-Methyle decaline
		1,2,3,4-Tetrahydro-naphthalene
		1,2,3,4-Tetrahydro-6-methyle naphthalene
		2,4-dimethyle-3-hexanone
Cetone	2-Pentadecanone	
	2-Heptadecanone	
	3-Octadecanone	
	2,6,10,14-Tetramethylepentadecan-3-one	
	Nonadecanone	

was used for this work. Test engine specifications are given in Table 4. The engine was mounted on a fixed table and coupled with an eddy current dynamometer that converts mechanical energy generated by the engine power directly to the net work. The schematic of test engine setup is shown in Fig. 1. Two systems were installed to manage the control and acquisition of measured

**Table 4**  
Specifications of test engine.

Make	Lister Petter
No of cylinder	One
Type of cooling	Air cooled
Bore × stroke	95.5 × 88.94 mm
Length of connecting rod	165.3 mm
Displacement	630 cm <sup>3</sup>
Fuel injection timing	20° bTDC
Fuel injection pressure	250 bar
Compression ratio	18:1
Rated power	4.5 kW @1500 rpm

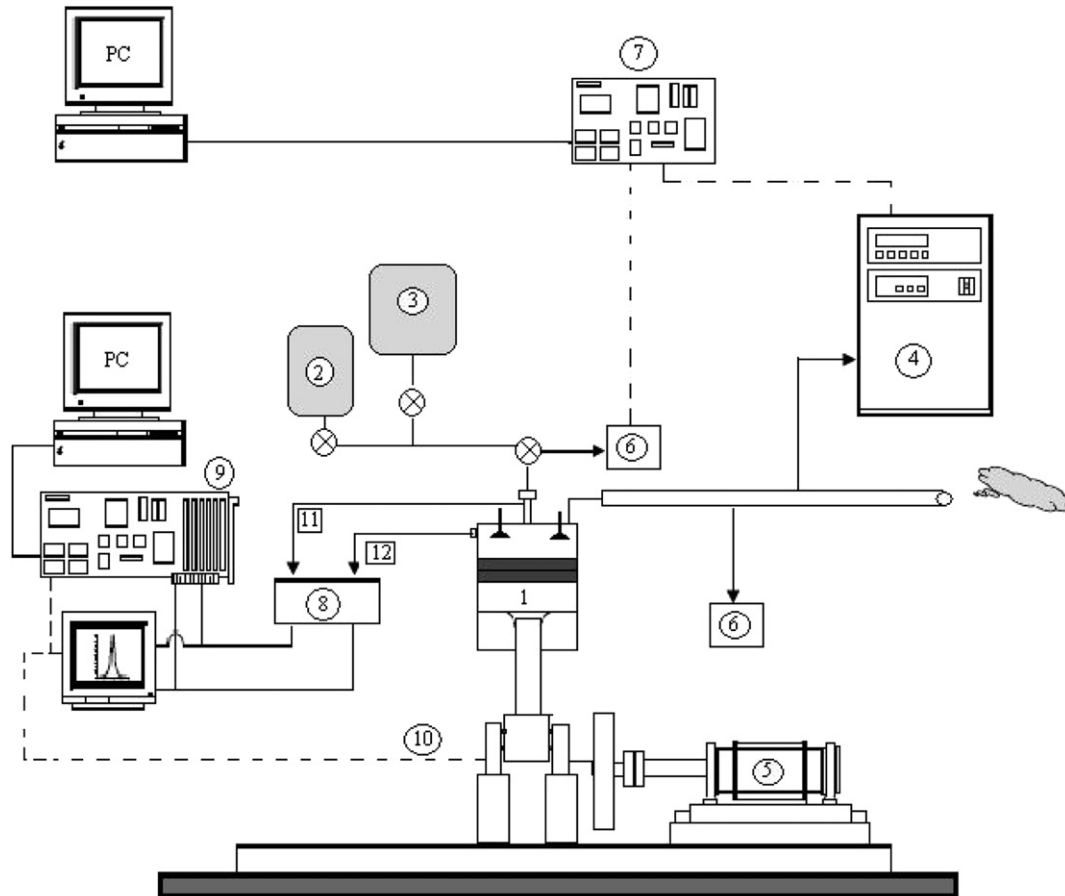
signals. First system controls the engine-dynamometer and also controls the acquisition of low-frequency measurements (torque, engine speed, pressure and temperature in the collectors). Second system measures high-frequency signal, which mainly concern the cylinder pressure, fuel injection pressure and also the angular position of the crankshaft. The pressure in the cylinder was measured at a frequency of 90 kHz using a piezoelectric pressure sensor, water cooled, type AVL QH32D. These signals are given to signal amplifying unit (National Instrument NIPXI-1050). A program was written in lab view 8.2 with 100 cycles average plot the value of pressure and crank angle with an accuracy in the order of tenths of degree.

The injection pressure was measured by a piezoelectric pressure transducer, type AVL QH33D, located in between the injection pump and the fuel injector. The angular position of the crankshaft was measured by an encoder, type AVL 364C, placed on the flywheel. The flow of intake air was measured by a differential pressure transmitter; type LPX 5481. For temperature measurements, the test engine was equipped with a series of thermocouples type K. Ambient temperature was measured by an active transmitter for humidity and temperature, type HD 2012 TC/150. The fuel flow was measured using a Coriolis mass flow meter. For measuring emissions, a bay of analysis (Crystal COSMA 500) placed on the line of engine exhaust gas was used to analyze the main pollutant gases. Emissions of hydrocarbons (HC) were measured by FID flame ionization using a heated hydrocarbon analyzer (model GRAPHITE 52M), emissions of nitrogen oxides (NO<sub>x</sub>) were measured via a chemiluminescence nitrogen oxide analyzer TOPAZE 32M. Emissions of carbon monoxide (CO) and oxygen (O<sub>2</sub>) were measured by absorption of infrared radiation using a 2M MIR analyzer. Particulate emissions were measured using a dust analyzer in real time (TEOM model 1105), for measurement and continuous weighing of the mass concentration of particulate exhaust. The experimental results of fuel flow rate, exhaust gas temperature, NO<sub>x</sub>, CO, O<sub>2</sub> and UHC were taken from 20 cycle average. The data acquisition system for these parameters was connected with Lab view 8.2 software which gave 20 cycle average. All the experiments were repeated five times to verify the performed measure.

## 4. Results and discussion

### 4.1. Performance parameters

The brake thermal efficiency with brake power for biofuel-diesel blends is compared with diesel and biofuel is shown in Fig. 2. The brake thermal efficiency is higher when biofuel is used as a neat fuel (B100) compared to blends. The brake thermal efficiency is 32.4% with neat biofuel at 80% of maximum load. This is mainly due to good hydrocarbon groups are present in biofuel compared to diesel which increase the rate of combustion. Also, higher cetane number of biofuel starts the combustion early, results more energy



- |                                 |  |
|---------------------------------|--|
| (1) Test Engine                 | (7) Low Frequency Data Acquisition System  |
| (2) Biofuel Tank                | (8) Charge Amplifier                       |
| (3) Diesel Fuel Tank            | (9) High Frequency Data Acquisition System |
| (4) Exhaust Gas Analyzer        | (10) Crank Angle Encoder/ Speed Sensor     |
| (5) Eddy Current Dynamometer    | (11) Injection Pressure Signal             |
| (6) Particulate Matter Analyzer | (12) Cylinder Pressure Signal              |

Fig. 1. Schematic diagram of the engine setup.

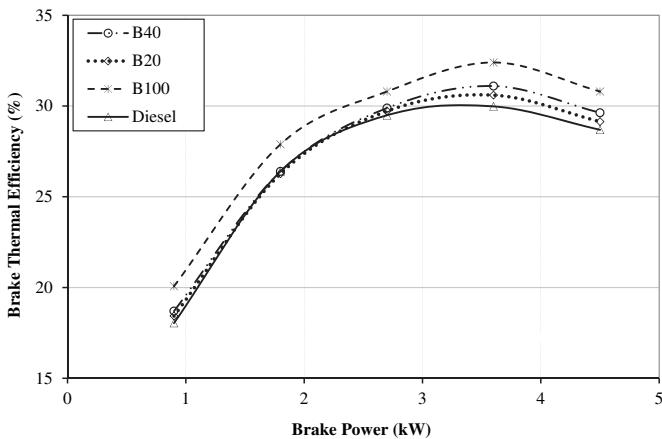


Fig. 2. Variation of brake thermal efficiency with brake power.

is released at the beginning of expansion stroke reflects higher mechanical output. The brake thermal efficiency increases with the blend of biofuel with diesel. The brake thermal efficiency is 31.1% with B40, 30.6% with B20 and 29.98% with neat diesel at 80% of maximum load. The increase in brake thermal efficiency with biofuel-diesel blend is due to the increase in fuel quality leads to higher premixed combustion compared to neat diesel. The brake thermal efficiency reduces slightly with all fuels at maximum load. It is 30.8% for neat biofuel, 28.69% for neat diesel, 29.63% for B40 and 29.14% for B20 at maximum load.

Fig. 3 shows the variation of exhaust gas temperature with brake power for biofuel, diesel and different blends of biofuel and diesel. The value of exhaust gas temperature for biofuel and diesel is 422 °C and 495 °C respectively at maximum load. The ignition delay and combustion duration is very short for biofuel which show that the ignition starts earlier and also combustion ends earlier than other test fuels. This is mainly due to the high cetane number and

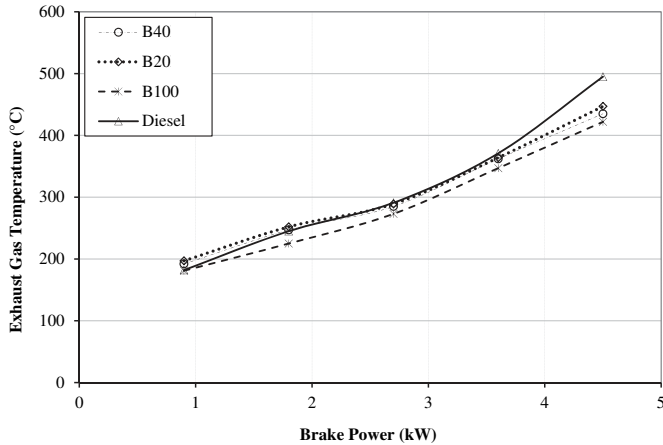


Fig. 3. Variation of exhaust gas temperature with brake power.

good combustion characteristics of biofuel. Hence, the amount the energy released at end of expansion stroke is less which leads to less exhaust gas temperature with neat biofuel. The value of exhaust gas temperature for B20 and B40 is 447 °C and 435 °C respectively. As the concentration of biofuel increases in the blend, the exhaust temperature decreases. This decrease in exhaust gas temperature than diesel is due to shorter ignition delay and combustion duration as compared to diesel, which show more amount of fuel burned during premixed combustion.

#### 4.2. Emission parameters

Fig. 4 shows the variation of  $\text{NO}_x$  emissions with brake power for different fuels. Oxides of nitrogen ( $\text{NO}_x$ ) in the exhaust emissions contain nitric oxide (NO) and nitrogen dioxide ( $\text{NO}_2$ ). It is very high with biofuel compared to all other fuels. The formation of  $\text{NO}_x$  is highly dependent on in-cylinder temperature, oxygen concentration which is 5.34% with biofuel and residence time for the reaction to take place. Also, the premixed combustion is very strong with biofuel which increases the combustion temperature. The premixed combustion is low and the diffusion combustion is high with diesel compared to biofuel which shows that the burning rate of diesel is low. The  $\text{NO}_x$  emissions at 80% of maximum load are 917 ppm with biofuel, 852 ppm with diesel, 882 ppm with B40 and 866 ppm with B20 blend. The results also show that the  $\text{NO}_x$  emissions are slightly low at maximum load with biofuel, diesel,

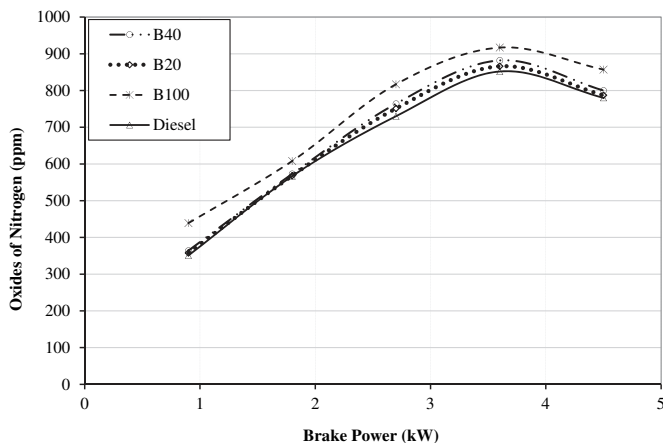


Fig. 4. Variation of oxides of nitrogen with brake power.

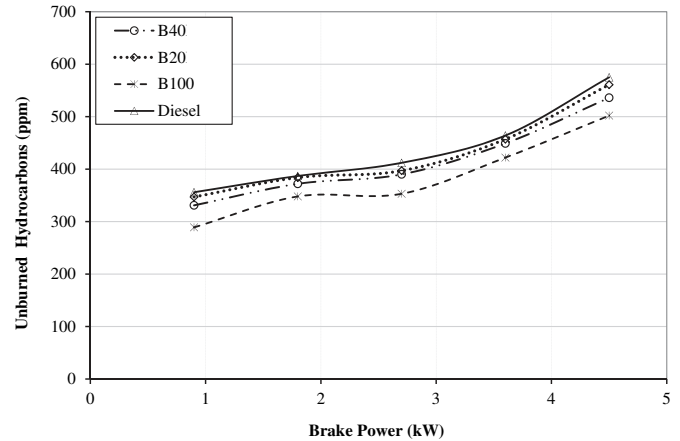


Fig. 5. Variation of unburned hydrocarbons with brake power.

B40 and B20 which has the value of 857 ppm, 780 ppm, 800 ppm and 787 ppm respectively.

Fig. 5 depicts the trends of UHC emissions with brake power for biofuel, diesel and different blends. It can be observed that UHC increase with an increase of load for all fuels. It is very low for biofuel at all loads compared to other fuels. This may be due to more oxygen molecules being present in the biofuel lead to better combustion, results less UHC. The UHC emissions for biofuel, neat diesel, B40 blend and B20 blend are 502 ppm, 575 ppm, 536 ppm and 561 ppm respectively at maximum load. This increase in UHC emissions with neat diesel is due to insufficient oxygen molecules present in the fuel for the oxidation process.

The variation of CO emission for different blends of diesel and biofuel is shown in Fig. 6. The CO emission for base diesel is 0.59%. It is decreased when the biofuel mixed with diesel. Biofuel is having higher concentration of oxygen content in the combustion gases which lead to greater oxidation than diesel fuel. The CO emission for B20 and B40 is 0.54% and 0.48% respectively at maximum load. It also shows that the decrease in CO emission with biofuel is higher compared to diesel and other blends and the value is 0.39%. This is mainly due to high concentration of oxygen in the biofuel leads to complete combustion.

Fig. 7 shows the variation of oxygen percentage for biofuel, diesel and other blends with brake power. The concentration of oxygen present in the engine exhaust is very low with biofuel. The biofuel is having higher oxygen content which is utilized maximum

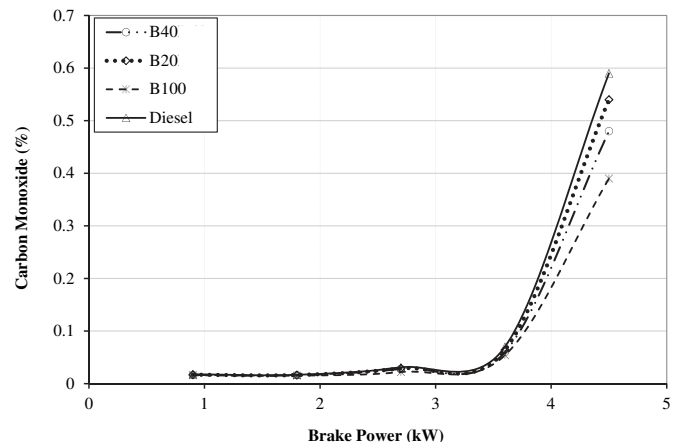


Fig. 6. Variation of carbon monoxide with brake power.

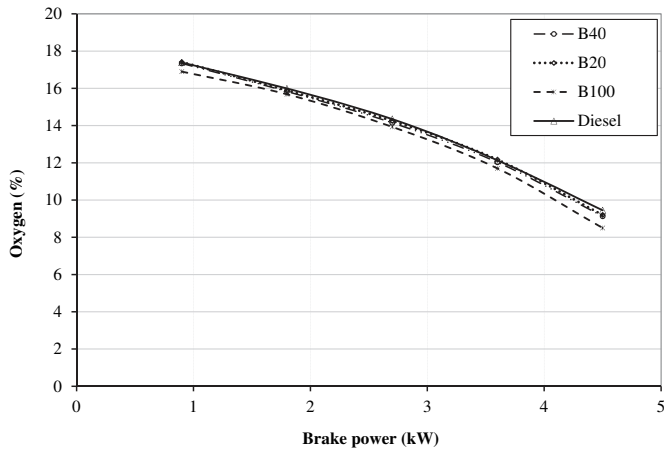


Fig. 7. Variation of oxygen with brake power.

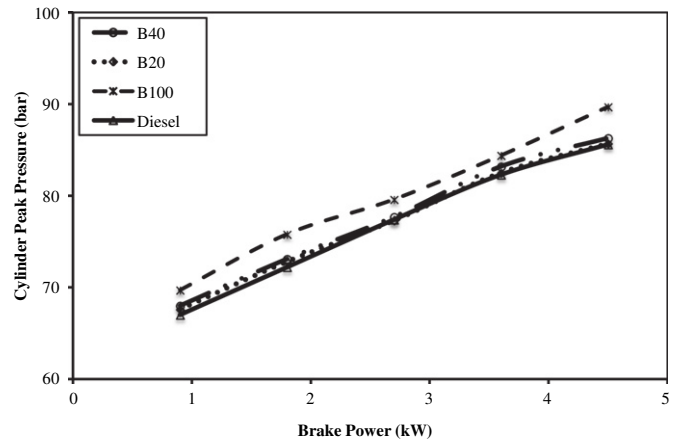


Fig. 9. Variation of cylinder peak pressure with brake power.

to make the combustion complete. The value of oxygen in the exhaust with biofuel operation is 8.5%. It is increased slightly with blends (B40 and B20). It is 9.13% and 9.2% with B40 and B20 respectively at maximum load. This is due to lesser quantity of oxygen is present in the fuel as well as in the combustion gases. The oxygen is very high with diesel and the value is 9.45%. The above results show that oxidation process is very good if the fuel is having oxygen content which enhance the combustion and reduce the pollutant emissions.

The variation of particulate matter (PM) emission with brake power for diesel, biofuel and their different blends is shown in Fig. 8. The carbon particles present in the exhaust is called particulate matter which is formed in the fuel rich pockets region present in the combustion chamber during combustion. The particulate matter is very high with diesel. It is reduced with the addition of biofuel with diesel. This clearly indicates that the biofuel exhibit a clean combustion. PM in a diesel engine is the function of amount of carbon and soot particles accumulated and are decided by intensity of diffusion combustion phase. The premixed combustion with diesel requires longer time to mix with oxygen which results the premixed combustion decreases and the diffusion combustion increases. PM emission for biofuel is very low compared to diesel. Higher percentage of oxygen improves vaporization of fuel and properly mixed with air attributes higher heat release rate during premixed combustion. Also, the diffusion combustion is less with biofuel compared diesel. The PM for diesel, biofuel, B20 and B40 is 8271 ng/s, 7842 ng/s, 8217 ng/s and 8137 ng/s respectively at maximum load.

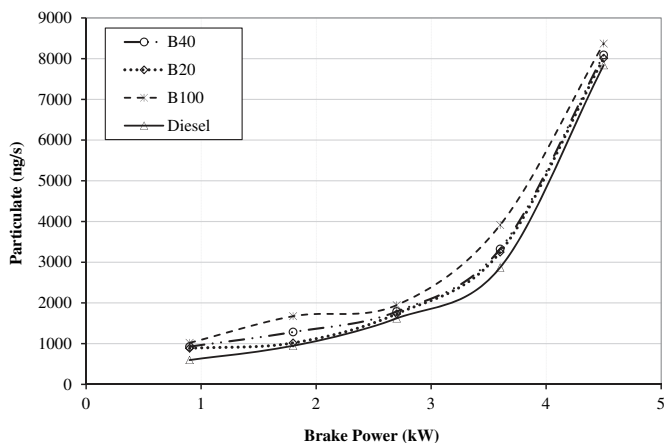


Fig. 8. Variation of particulate matter with brake power.

#### 4.3. Combustion parameters

The variation of cylinder peak pressure with brake power is shown in Fig. 9. It is clear that cylinder peak pressure varies with load. It is because of the combustion is very fast when load increases. The cylinder peak pressure for diesel is 85.6 bar at maximum load. The addition of biofuel in the blend increases the cylinder pressure at all loads. The increase in peak pressure is noticed with blends, it is 85.7 bar with B20 blend and 86.3 bar with B40 at maximum power. This is mainly due to the addition of biofuel with diesel increases the oxygen concentration in the blend. This enhances combustion rate on account of the flame propagation through the biofuel addition. The cylinder pressure is maximum with neat biofuel and the value is about 89.7 bar.

The variation of cylinder pressure with crank angle at maximum load for biofuel, diesel and different blends is shown in Fig. 10. The injected fuel is being mixed with air which attains the auto ignition temperature, the combustion will start and releases energy. This energy is utilized to increase the in-cylinder pressure. From this the occurrence of maximum pressure is mainly depends on fuel mixing rate. The biofuel blends having higher oxygen concentration due to that high mixing rate leads the combustion starts earlier than diesel. The occurrence of maximum pressure for B20 and B40 is 5.9°CA after TDC and 5.5°CA after TDC. But for neat diesel it is about 6.1°CA after TDC. This is too early with biofuel is about 4.3°CA after TDC.

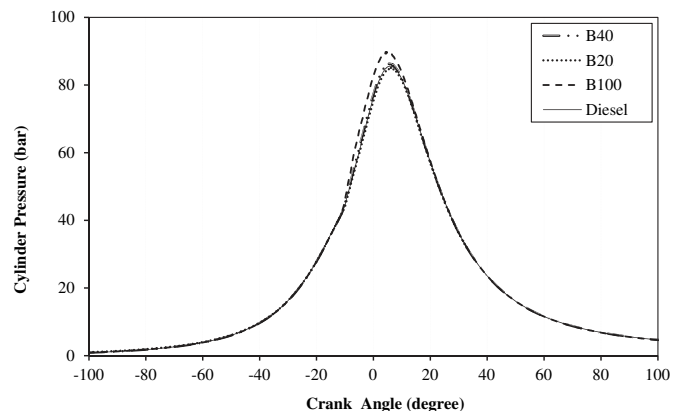


Fig. 10. Variation of cylinder pressure crank angle at maximum load.

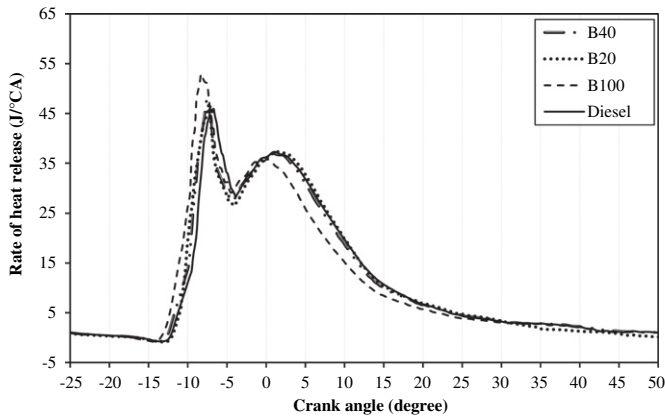


Fig. 11. Variation of heat release rate with crank angle at maximum load.

Fig. 11 shows the variation of rate of heat release with crank angle at maximum load for biofuel, diesel and different blends of biofuel and diesel. Diesel has very low premixed combustion and high diffusion combustion. Premixed combustion is mainly depends on how much amount of fuel is taken part in the initial phase of combustion. This mainly depends on following factors; presence of oxygen, air fuel mixing rate and cetane number. The presence of oxygen during combustion with diesel is low compared to biofuel and its blends. This leads to lower air fuel mixing rate and also low cetane number (compared to biofuel) starts the combustion late. Due to that the maximum premixed combustion is at 7.1°CA before TDC and more amount of fuel is burned during diffusion combustion. The rate of combustion increases with concentration of biofuel increases in the blend. Also, the maximum premixed combustion for biofuel is earlier than diesel. This is about 7.3°CA before TDC with B20 and 7.5°CA before TDC with B40. The presence of oxygen in the biofuel increases the rate of combustion with these blends. The occurrence of maximum premixed heat with neat biofuel is at 8.3°CA before TDC. Also, the quantity of fuel burned during premixed combustion is very high and diffusion combustion is very low compared to all other fuels.

Fig. 12 depicts the variation of ignition delay with brake power for biofuel, diesel and its blend. It is found that the ignition delay increases when the engine load increases. This is due to the influence of cylinder gas temperature which is lower at the low engine loads and increases at high engine loads. The ignition delay is

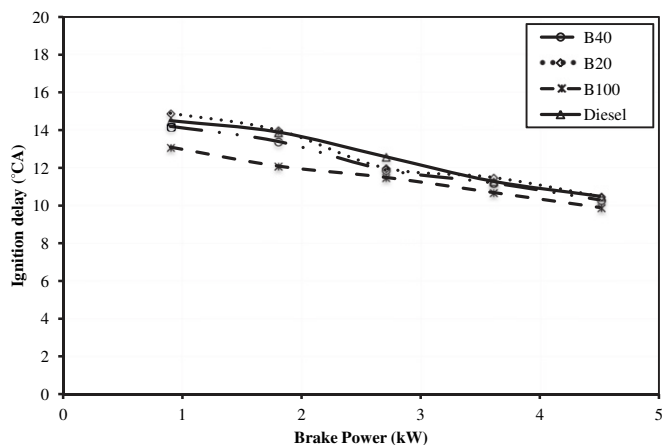


Fig. 12. Variation of ignition delay with brake power.

higher for neat diesel; it is 10.5°CA at maximum load. It decreases with the increase in biofuel mass fraction in the blend. The decrease in ignition delay with increase of the biofuel concentration is due to higher cetane number and higher oxygen concentration of the blend. This increases the fuel evaporation, easily mixes with oxygen and starts the combustion earlier. The value for the different blends is 10.5°CA for B20 and 10.3°CA B40. The ignition delay reduces to the minimum of 9.9°CA with neat biofuel.

The variation of combustion duration for biofuel, diesel and different blends of diesel and biofuel with respect to brake power is shown in Fig. 13. The combustion duration is higher for diesel compared to biofuel and the value is 44.7°CA at maximum load. The combustion duration decreases with diesel/biofuel blends. The combustion duration for B20 and B40 is 44°CA and 43.2°CA respectively at maximum load. The oxygen present in the blend increases the air fuel mixing rate tends to increase the amount of fuel being prepared during the initial stage of combustion (pre-mixed combustion). This increases the premixed combustion and reduces the diffusion combustion. It is maximum with neat biofuel (41.2°CA) compared to all other test fuels. This may be due to higher concentration of alkene group of hydrocarbons and cetane number of the biofuel starts and ends the combustion earlier.

## 5. Estimation of uncertainty

While measuring any quantity, the results will always differ from the true value even with careful experimentation. This error in measurement may be either random or systematic. By adding a correction value, the systematic error can be removed. Random error can only be estimated statistically and cannot be predicted in advance. Its presence can be detected only when the same quantity is measured again and again under the same conditions and with care.

The uncertainty was estimated based on Gaussian distribution method with confidence level of  $\pm 2\sigma$  (95.45% of measured data lie within the limits of  $\pm 2\sigma$  of mean). Thus uncertainty is estimated using the following equation.

$$\text{Uncertainty of any measured Parameter } (\Delta X) = 2\sigma i / \bar{X} * 100 \quad (1)$$

Experiments were conducted to obtain the mean ( $\bar{X}$ ) and standard deviation ( $\sigma$ ) of any measured parameter ( $X_i$ ) for 20 readings. From the measured parameters, the uncertainty is computed based on Kline and McClintock method [23].

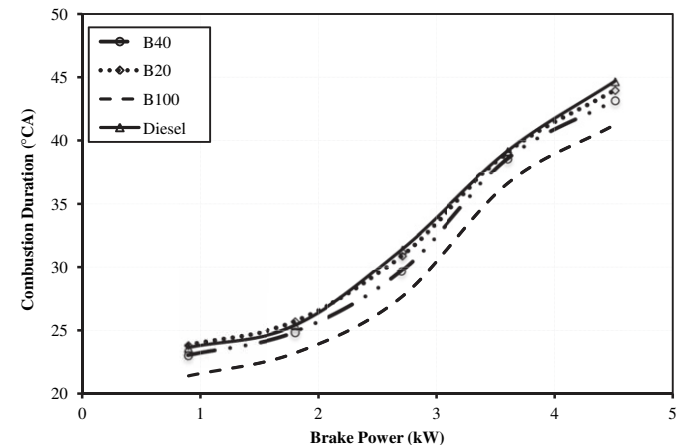


Fig. 13. Variation of combustion duration with brake power.



Let  $R$  be the computed quantity from  $n$  independent measured parameters

$$X_1, X_2, X_3, \dots, X_n$$

$$\text{Thus } R = R(X_1, X_2, X_3, \dots, X_n) \quad (2)$$

Let uncertainty limits for the measured parameters be

$$X_1 \pm \Delta X_1, X_2 \pm \Delta X_2, X_3 \pm \Delta X_3, \dots, X_n \pm \Delta X_n$$

and the uncertainty limit for the computed value be  $R \pm \Delta R$ .

In order to get the realistic error limits for any computed quantity based on several measured quantities the principle of root-sum-square method is used and the magnitude of the error is given by

$$\Delta R = \text{SQRT} \left( (\partial R / \partial X_1 * \Delta X_1)^2 + (\partial R / \partial X_2 * \Delta X_2)^2 + \dots + (\partial R / \partial X_n * \Delta X_n)^2 \right) \quad (3)$$

Using the equation (3) the uncertainty for a given operating condition was computed.

The estimated uncertainty values at different operating conditions are

Brake power: 0.4–1.7%  
 Specific fuel consumption: 0.5–1.9%  
 Brake thermal efficiency: 0.6–1.9%

The sensitivity of the various instruments is given in Table 5.

**Table 5**  
 Sensitivity of instruments used.

Parameter	Sensor type	Error
Torque ( $T_m$ )	Effort sensor (FN 3148)	$\pm 0.1$ N m
Engine speed	AVL 364C	$\pm 3$ RPM
Injection timing	AVL 364C	$\pm 0.05^\circ$ CA
Intake air flow rate	Differential pressure transmitter (LPX5841)	$\pm 1\%$ of measured value
Fuel flow rate	Coriolis type mass flow meter (RHM015)	$\pm 0.5\%$ of measured value
In-cylinder pressure	Piezo-electric (AVL QH32D)	$\pm 2$ bars
Injection pressure	Piezo-electric (AVL QH33D)	$\pm 2.5$ bars
Intake air temperature	Differential pressure transmitter (LPX5841)	$\pm 1.6$ K
Fuel injection temperature	K type thermocouple	$\pm 1.6$ K
Exhaust gas temperature	K type thermocouple	$\pm 1.6$ K
Ambient air temperature	HD 2012 TC/150	$\pm 0.2$ K
Relative humidity	HD 2012 TC/150	$\pm 2\%$
Hydrocarbon emissions	FID (GRAPHITE 52M)	$\pm 10$ ppm
Nitric oxides emissions	TOPAZE 32M	$\pm 100$ ppm
Carbon dioxide emissions	Infra-red detector (MIR 2M)	$\pm 0.2\%$
Non-reacted oxygen	Infra-red detector (MIR 2M)	$\pm 0.25\%$
Carbon monoxide emissions	Infra-red detector (MIR 2M)	50 ppm
Particulate matter emissions	TEOM 1105	$\pm 10$ ng/s
Fuel lower heating value	Isoperibol calorimeter (PARR 6200CLEF)	$\pm 0.25\%$ of measured value

## 6. Conclusions

From experimental work it is observed that the engine was running very smoothly with biofuel derived from fish oil industrial residue and its blends. The brake thermal efficiency increases to 32.4% with biofuel which is 2.42% higher than diesel. It is 30.6% and 31.1% with B20 and B40 respectively. The HC and CO emissions for diesel, B20 and B40 is 575 ppm and 0.59%, 561 ppm and 0.54% and 536 ppm and 0.48% respectively at maximum load which shows biofuel blends produces less HC and CO emissions compared to diesel. The particulate emissions reduced for blends than diesel. But there is a slight increase in  $\text{NO}_x$  emissions with biofuel and its blends than diesel. Remedies should be taken to reduce this emission. From the performance, emission and combustion characteristics of diesel engine with biofuel and its blends, it is concluded that the biofuel from fish oil industrial residue by catalytic cracking can be the substitute for diesel fuel.

## Acknowledgments

GEPEA Laboratory and the Department of Energetic and Environmental Systems (DSEE), supported this research at the École des Mines de Nantes. These supports are gratefully acknowledged.

## References

- Escobar José C, Lora Electo S, Venturini Osvaldo J, Yáñez Edgar E, Castillo Edgar F, Almazan Oscar. Biofuels: environment, technology and food security. *Renewable Sustainable Energy Review* 2009;13:1275–87.
- He Y, Wang S, Lai KK. Global economic activity and crude oil prices: a cointegration analysis. *Energy Economics*; 2010.
- Dahlquist Erik, Thorin Eva, Yan Jinyue. Alternative pathways to a fossil-fuel free energy system in the Mälardalen region of Sweden. *International Journal of Energy Research* 2007;31:1226–36.
- Rakopoulos CD, Antonopoulos KA, Rakopoulos DC, Hountalas DT, Giakoumis EG. Comparative performance and emissions study of a direct injection diesel engine using blends of diesel fuel with vegetable oils or biodiesels of various origins. *Energy Conversion and Management* 2006;47:3272–87.
- Misra RD, Murthy MS. Straight vegetable oils usage in a compression ignition engine—a review. *Renewable and Sustainable Energy Reviews* 2010;14:3005–13.
- Karthikeyan B, Srithar K. Performance characteristics of a glowplug assisted low heat rejection diesel engine using ethanol. *Applied Energy* 2011;88:323–9.
- Kusaka Jin, Daisho Yasuhiro, Kihara Ryoji, Saito Takeshi. Combustion and ignition characteristics in a glow assisted methanol DI engine (optimization of slit geometries and glow-plug temperature). *JSAE Review* 1997;18:64–6.
- Quintero JA, Montoya MI, Sánchez OJ, Giraldo OH, Cardona CA. Fuel ethanol production from sugarcane and corn: comparative analysis for a Colombian case. *Energy* 2008;33:385–99.
- Mekhilef S, Siga S, Saidur R. A review on palm oil biodiesel as a source of renewable fuel. *Renewable and Sustainable Energy Reviews* 2011;15:1937–49.
- Demirbas Ayhan. Combustion characteristics of different biomass fuels. *Progress in Energy and Combustion Science* 2004;30:219–30.
- Wisniewski Jr A, Wiggers VR, Simionatto EL, Meier HF, Barros AAC, Madureira LAS. Biofuels from waste fish oil pyrolysis: chemical composition. *Fuel* 2010;89:563–8.
- Andersen Otto, Weinbach Jan-Erik. Residual animal fat and fish for biodiesel production. *Potentials in Norway. Biomass and Bioenergy* 2010;34:1183–8.
- Taufiqurrahmi Niken, Mohamed Abdul Rahman, Bhatia Subhash. Production of biofuel from waste cooking palm oil using nanocrystalline zeolite as catalyst: process optimization studies. *Bioresource Technology* 2011;102:10686–94.
- Arpa Orhan, Yumrutas Recep, Demirbas Ayhan. Production of diesel-like fuel from waste engine oil by pyrolytic distillation. *Applied Energy* 2010;87:122–7.
- Bezergianni Stella, Kalogianni Aggeliki. Hydrocracking of used cooking oil for biofuels production. *Bioresource Technology* 2009;100:3927–32.
- Karagöz Selhan. Energy production from the pyrolysis of waste biomasses. *International Journal of Energy Research* 2009;33:576–81.
- ShiungLam Su, Russell Alan D, Chase Howard A. Microwave pyrolysis, a novel process for recycling waste automotive engine oil. *Energy* 2010;35:2985–91.

- [18] Vamvuka D. Bio-oil, solid and gaseous biofuels from biomass pyrolysis processes—an overview. *International Journal of Energy Research* 2011;35:835–62.
- [19] Adebajo Adenike O, Dalai Ajay K, Bakhshi Narendra N. A production of diesel-like fuel and other value-added chemicals from pyrolysis of animal fat. *Energy and Fuels* 2005;19:1735–41.
- [20] Dos Anjos JoséRibamar Segundo, Araujo Gonzalez Wilma De, Lam Yiu Lau, Frety Roger. Catalytic decomposition of vegetable oil. *Applied Catalysis* 1983; 5:299–308.
- [21] Zhang Qi, Chang Jie, Wang Tiejun, Xu Ying. Review of biomass pyrolysis oil properties and upgrading research. *Energy Conversion Management* 2007;48: 87–92.
- [22] Blin Joël, Volle Ghislaine, Girard Philippe, Bridgwater Tony, Meier Dietrich. Biodegradability of biomass pyrolysis oils: comparison to conventional petroleum fuels and alternatives fuels in current use. *Fuel* 2007;86:2679–86.
- [23] Kline SJ, McClintock FA. Describing uncertainties in single sample experiments. *Mechanical Engineering* 1953;3.